Interaction of a Spin-Labeled Adenine−Acridine Conjugate with a DNA Duplex Containing an Abasic Site Model†

Fabrice Thomas, Josette Michon,* and Jean Lhomme

L.E.D.S.S., Chimie Bioorganique, UMR CNRS 5616, Université Joseph Fourier, BP 53, 38041 Grenoble Cedex 9, France

Received July 22, 1998; Revised Manuscript Received November 6, 1998

ABSTRACT: The abasic site is a common lesion in DNA that is also formed as an intermediate in the base excision repair of damaged bases. We have previously reported the adenine−acridine conjugate **1** that was designed to bind to the abasic site and interfere with the repair process. High-field NMR had shown that **1** forms specific complexes with a DNA duplex containing an apurinic abasic site model. We report here the dynamics of the interaction of the nitroxide-labeled analogue **3** of the conjugate **1** with the same apurinic oligonucleotide and with the parent unmodified duplex. Identical study of the labeled acridine subunit **5** used as a reference is also reported. In the presence of the apurinic duplex and depending on the concentrations and drug ratios, three species are observed: the radical "free in solution", the "intercalation" complex characterized by its similarity to that observed in the presence of the parent unmodified duplex, and the "abasic-site-specific" complex which is the sole species visible at low drug ratios. The experimental data reinforced by molecular modeling of the complex and theoretical calculation of correlation times suggest (i) the most immobilized form corresponds to that observed by NMR and (ii) complexation of the drug is little or not modified by the spin-label. We also show that the abasic site constitutes a binding site for the propylaminoacridine intercalator **5**.

Abasic sites (apurinic/apyrimidinic sites: AP[1] sites) are common lesions in DNA and also constitute important intermediates in the repair of DNA base damages (*1*). AP site lesions are produced spontaneously by hydrolysis of the N-glycosidic bond under physiological conditions (*2*). The purine glycosidic bond is most susceptible to hydrolysis, and guanine is released slightly more rapidly than adenine (*3*). Chemical modification of the bases by carcinogens, or by alkylating agents (*1*), or by ionizing radiation (*4*) that destabilizes the N-glycosidic bond promotes formation of abasic sites. For example, by alkylation of purinic bases, essentially at N-7, the depurination rate is accelerated by ca. 10^6-fold (*1*). Some alkylating anticancer agents, such as the nitrosoureas, produce abasic sites at high frequencies in the cell, and their toxicity has been associated with abasic site formation (*5*). AP sites are also generated enzymatically as intermediates in the repair of damaged or abnormal bases in the base excision repair (BER) process. Two major classes of repair enzymes incise DNA at abasic sites. Class I AP-endonucleases, also known as AP-lyases, cleave the 3′-phosphodiester bond of the AP site by a β-elimination mechanism, leaving an $\alpha-\beta$ unsaturated aldose 5-phosphate (*6*). Class II AP-endonucleases cleave hydrolytically the phosphodiester bond 5′ to the AP site, producing a 3′-OH nucleotide and a 5′-phosphate deoxyribose residue (*7*). If not repaired, abasic sites are strong blocks to DNA synthesis and constitute lethal lesions (*8*). Translesional DNA synthesis may also occur with low frequency, resulting in mutation (*9*, *10*).

In view of the biological significance of AP sites as intermediates in the repair of damaged DNA and as toxic lesions created notably by alkylating anticancer agents, there is considerable challenge in targeting this lesion by synthetic molecules. In a general program aimed at designing molecules that could recognize specifically the abasic site in DNA and possibly interfere with the repair process, we prepared a series of molecules that mimic the action of AP-endonucleases of the AP-lyase class, i.e., molecules that recognize the abasic site and incise DNA by a β-elimination mechanism (*11*−*15*). The molecules include an acridine intercalating moiety for strong interaction with DNA, a nucleic base as recognition unit to pair with the base opposite the abasic site, and a polyamino linking chain endowed with two functions, ionic binding to the phosphates involving one protonated amino site and cleavage catalysis through one unprotonated nitrogen (Scheme 1). The number of methylenes separating the amino functions controls the pK_a of the two aforementioned amines in the linker (*16*). The most efficient molecules cleave plasmid pBR322 DNA containing an average of 1.7 abasic sites in its 4260 bp sequence at nanomolar concentrations and thus behave as lyase mimics in terms of selectivity and efficiency (*13*). More recently these molecules were shown to act as inhibitors of the base excision repair (BER) mechanism and quite interestingly to sensitive cells to the alkylating antitumor agent BCNU whose mode of action has been associated with its ability to create abasic sites at high frequencies in the cell (*17*). It is worth noting that in the whole series of molecules examined, those

† This work was supported by the Association pour la Recherche sur le Cancer (ARC), the Ligue Nationale contre le Cancer, and the Région Rhône-Alpes.

* To whom correspondence should be addressed.

[1] Abbreviations: AP, apurinic/apyrimidinic; BER, base excision repair; BCNU, *N*,*N*′-bis(2-chloroethyl)-*N*-nitrosourea; EDTA, ethylenediaminetetraacetic acid; DMSO, dimethyl sulfoxide.

10.1021/bi981770e CCC: $18.00
Published on Web 01/20/1999

Scheme 1

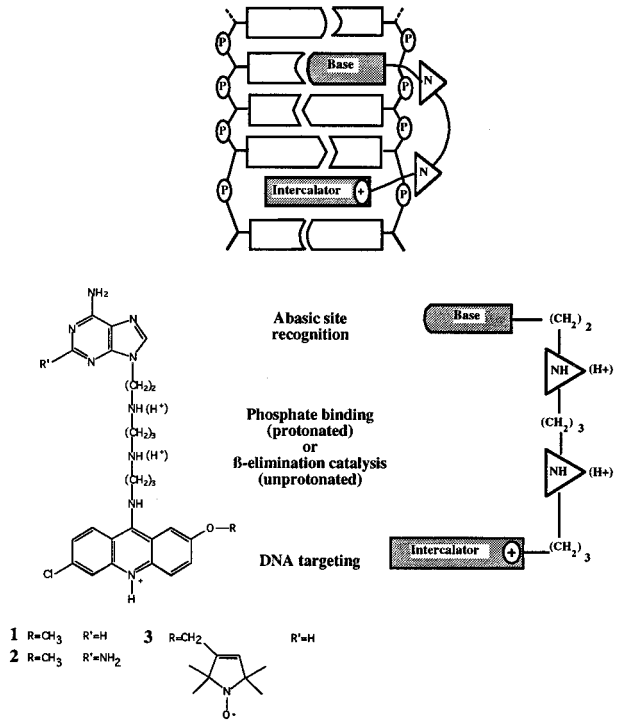

two derivatives, **1** and **2**, that show the highest cleavage efficiency equally behave as the best inhibitors of the base excision pathway (*13*). To get a clear picture of the mode of interaction of molecules **1** and **2** at the abasic site, we conducted a high-field NMR study of the complex formed with a synthetic oligonucleotide possessing a stable analogue of the abasic site and a thymine residue opposite the apurinic site (*18*). The 500 and 600 MHz NMR coupled to molecular modeling examination of the drugs in association with the oligonucleotide indicated the presence of two complexes in which the purine base of the drug inserts into the abasic pocket pairing with thymine in the opposite strand, most probably in the HOOGSTEEN mode, the acridine intercalates at a two base pair distance 5′ to the abasic site, and the polyamino chain lies in the minor groove. The two complexes differ by a 180° rotation of the acridine ring around the C9−N bond (*19*). Thermal denaturation studies monitored by UV spectroscopy also demonstrated stabilization of the abasic duplex by conjugates **1** and **2**, indicating specific binding to the abasic site (*20*). To get dynamic information of those complexes, we turned to EPR spectroscopy.

EPR is a technique that proved successful to study dynamic processes in the milli- to nanosecond time regime. The first studies in the nucleic acid field involved spin-labeled tRNA (*21*, *22*). DNA dynamics were next examined using both enzymatic and chemical incorporation of the spin-label in the polymer (*23*−*25*). More recently, development of automated chemical oligonucleotide synthesis allowed incorporation of spin-labeled nucleosides at preselected positions in the sequence (*26*−*31*). Covalently attached nitroxide spin-labeled psoralen derivatives were also evaluated as probes for DNA oligonucleotide dynamic studies (*32*). Information on the structure and local environment could thus be obtained through anisotropic motion of the spin-labels detected by EPR. Characteristic line shapes for particular nucleic acid conformations could be observed, including single strands, double-stranded A, B forms, and hairpin loops (*33a*). Z-DNA conformations were also detected by EPR (*33b*). In all these studies, the nature of the nitroxide spin-label and the position, size, and nature of the tether on the nucleic base are critical for the spin-label to correlate its motion with that of the attached base and report the global tumbling of the oligo- or polynucleotides (*29*). For example, in a 14-mer duplex containing a spin-labeled quinolone derivative, the 7.6 ns correlation time was in good agreement with the 7 ns value predicted by hydrodynamic theory (*34*). Hearst (*32*) has shown that for 25-mers, the approximation of isotropic rotation is very poor in this case. For quantifying the motion of spin-labeled bases within DNA, two models have been used: a dynamic cylinder model and a base disk model (*30*). In each model, the nitroxide motion consists of global and internal contributions. The interactions of noncovalently bound drug molecules with DNA have also been examined by EPR using spin-labeled analogues, including acridine derivatives (*35*, *36*), propidium (*37*), ethidium (*38*), oxazolopyridocarbazole (*39*), ruthenium complexes (*40*), and carcinogenic aromatic amines (*41*, *42*). Correlation times varying in a wide range (2−40 ns) were determined depending on the position of the label on the drugs and on the relative motions of the drugs and the DNA to which they are bound. Different modes of binding (intercalative and surface) corresponding to different correlation times (respectively 3 and 2 ns) could be evidenced in the interaction of nitroxide-substituted ruthenium complexes with DNA (*40*). EPR spectroscopy necessitates spin-labeling of the drug to be examined with the requirement that the label modifies to a lesser extent the interaction properties of the drug. We recently observed that replacement of the methyl group in 2-methoxy-6-chloro-9-aminoacridine derivatives by a methylene pyrroline-1 oxyl group at carbon C-2 (Scheme 1) only modifies slightly the association constant of the molecule with calf thymus DNA (*43*). The spin-labeled adenine−acridine conjugate **3** can thus be considered as a good analogue of the unlabeled drug **1** that has been shown to complex quite selectively at the abasic site by high-field NMR spectroscopy (*19*).

We report in the present paper the EPR study of the interaction of the spin-labeled molecule **3** with the abasic oligonucleotide previously examined by NMR (*18*) that we note "duplex TX". The target oligonucleotide possesses the following structure:

5′d(CGCAC**X**CACGC)3′
3′d(GCGTGTGTGCG)5′

in which X is a "classical" model abasic site, i.e., the 3-hydroxy-2-hydroxymethyltetrahydrofuran moiety replacing deoxyribose for stability reasons (Scheme 2). For comparison, we present the EPR data of the complex formed with the parent "natural" duplex, noted [TA]. The same study was achieved with the labeled acridine subunit **5** used as a reference (Scheme 3). We show that the EPR data are quite complementary to the NMR data. In addition, EPR indicates the presence of minor complexes that could not be detected in the NMR analysis.

MATERIALS AND METHODS

Materials. Molecules **1**−**6** (*13*, *43*) and the abasic site-containing DNA undecamer (*18*) were synthesized and purified as reported previously.

Scheme 2

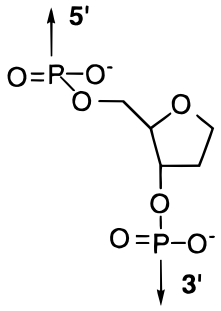

Abasic site analog (X)

Scheme 3

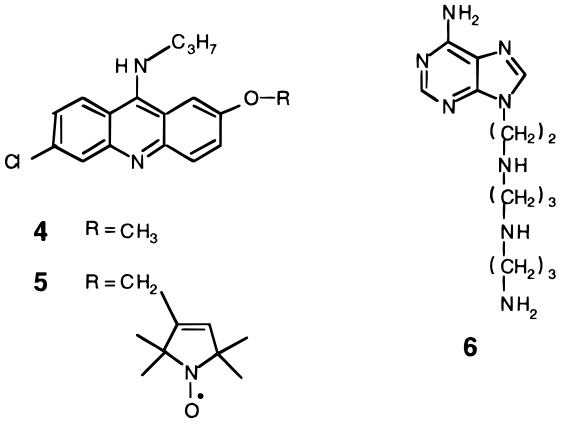

Electron Paramagnetic Resonance (EPR). The EPR spectra were performed on a Bruker ESP 300 E spectrometer operated in the continuous wave (CW) mode. For oligonucleotide binding studies, compounds **3** and **5** were solubilized in DMSO and then diluted in buffer (25 mM Tris-HCl, pH 7.0, 0.1 M NaCl, and 0.2 mM EDTA); the final concentration of DMSO was 2%. The concentration of oligonucleotide duplex (TA) was 1.03×10^{-5} or 4.56×10^{-5} M, and that of the tested drug **3** varied from 0.5×10^{-5} to 5×10^{-5} M. The concentration of abasic duplex (TX) was 0.91×10^{-5} or 2.36×10^{-5} M, and that of the tested drug **3** varied from 0.1×10^{-5} to 5×10^{-5} M. For drug **5**, the concentration was 2×10^{-5} M, and the concentration of oligonucleotide TX was 0.91×10^{-5} or 4.55×10^{-5} M and that of TA was 4.56×10^{-5} M. Analysis of spectra corresponding to several species was monitored using the Compare Menu of ESP 300E: when recording a spectrum of several species with different mobilities and having the spectra of the individual pure species, the pure spectra can be successively subtracted from the mixture. When the line shapes are different, if oversubtraction of the sharp lines corresponding to free species in buffer solution, for example, occurred, the sharp lines are phase-reversed. In this case, the end point is relatively precise. When the line shapes are related more closely, the end point becomes progressively harder to estimate. To obtain the integrated intensity of an EPR signal, double integration must be performed using the Integrate Menu of ESP 300 E. The integrated intensity is fairly immune to noise. The random fluctuations tend to cancel under integration. Integration, however, is very sensitive to base-line effects. Fortunately, such effects are easily corrected by base-line subtraction made in the program.

EPR Line Shape Theory. There are three parameters useful in nitroxide spin-label spectra: the **g** tensor, the nitrogen hyperfine coupling tensor **A**, and the widths of the individual EPR lines.

Analysis of rigid-limit X-band spectra gives values for the principal tensor elements $\mathbf{A}_{ZZ}$ and $\mathbf{g}_{ZZ}$. These values can be obtained since the upfield and downfield *Z*-turning points do not overlap with the other resonance peaks.

The EPR spectra are sensitive to nitroxide rotational motions. For example, in a nonviscous solvent, EPR spectra of nearly all nitroxides have three sharp lines of nearly equal height. This is due to rapid isotropic tumbling motion which averages away all anisotropic effects. In the case 10^{-11} s $< \tau_c < 10^{-9}$ s, the EPR spectrum gives dynamic information by measuring the heights and peak widths of the lines using Kivelson's formula (*44*): $\tau_c = C\Delta H_{(+1)}[\sqrt{h_{(+1)}/h_{(-1)}} - 1]$. $\Delta H_{(+1)}$ is the peak-to-peak line width expressed in gauss of the derivative of the low-field absorption line (corresponding to the nuclear magnetic moment $m_I = +1$). $h_{(+1)}$ and $h_{(-1)}$ are the corresponding peak heights for the low- and high-field lines, respectively. The constant *C* can be calculated from the principal values of **g** and **A** tensors of the nitroxide radical, $C = 6.6 \times 10^{-10}$, using published data for di-*tert*-butylnitroxide (*45*). This value does not change much between various nitroxide radicals. For large correlation times, Kuznetsov et al. (*46*) base their calculations of the spectra of a radical in a viscous isotropic medium on the assumption that changes in the orientation of the radical occur by means of random jumps. The time between two consecutive jumps is taken as the rotational correlation time. The low-field extremum of the first-derivative spectrum is shifted in the slow motional region, and it is convenient to use the parameter $X = [H(\tau_c) - H(\tau_c \rightarrow 0)]/[H(\tau_c \rightarrow \infty) - H(\tau_c \rightarrow 0)]$ where $H(\tau_c)$ is the position of the low-field maximum ($M = +1$) of the first-derivative spectrum and $H(\tau_c \rightarrow \infty)$ and $H(\tau_c \rightarrow 0)$ are the positions of this maximum for the two limiting values of τ_c. It is possible to obtain the rotational correlation time by plotting the dependence of the *X* parameter on τ_c. The small hydrodynamic anisotropy of a 11-mer suggests that a model assuming isotropic rotational motion may be reasonable. A more detailed and accurate analysis based on anisotropic tumbling was not performed in this study (*47*). To estimate the hydrodynamic properties of DNA, the DNA oligomers can be modeled as rigid cylinders with a radius $R = 12$ Å and a length of $3.4\ N$ Å where *N* is the number of base pairs (*48*, *26*). In the present case of the drug/11-mer complex, we used the value $N = 12$, considering that contribution of the intercalating drug to the length of the cylinder could be assimilated to that of a base pair.

Molecular modeling calculations were carried out and structures visualized on an IBM RS 6000-39H. Computer running DISCOVER and Insight II version 95.0 (M.S.I., Parc Club Orsay University 91830) were used.

RESULTS

*Interaction of **3** and **5** with the Natural TA Duplex.* The EPR spectra of the labeled aminoacridine **5** and the AP-lyase mimic **3** were registered in buffered aqueous solution at room

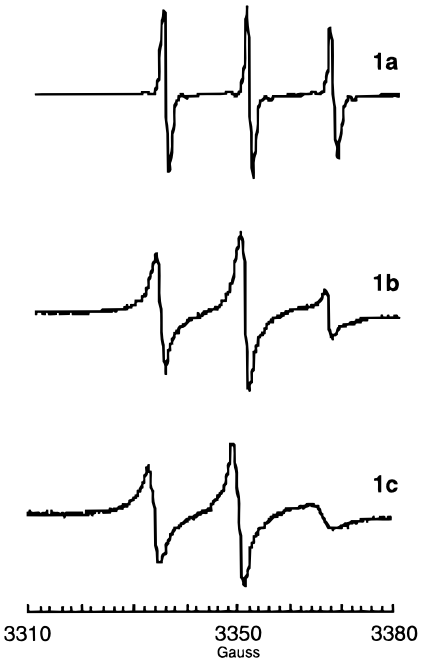

FIGURE 1: EPR spectra of (a) **3**, 2.5×10^{-5} M, 25 mM Tris−HCl, pH 7.0, 0.1 M NaCl, and 0.2 mM EDTA with 2% DMSO; (b) **3**, 2.5×10^{-5} M, in the presence of oligonucleotide TA, 4.56×10^{-5} M; (c) subtraction of spectrum 1a from spectrum 1b.

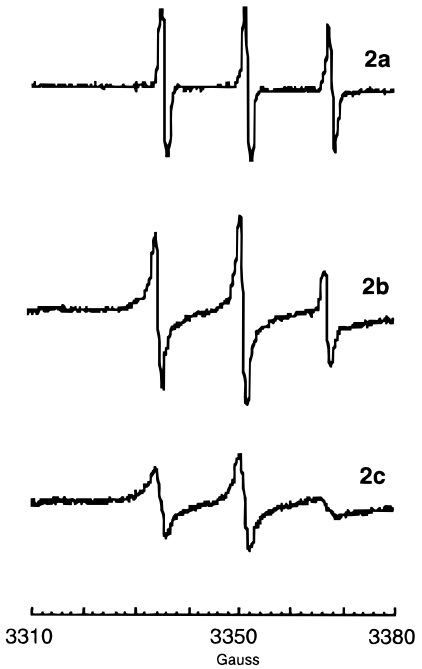

FIGURE 2: EPR spectra of (a) **5**, 2×10^{-5} M, in 25 mM Tris-HCl, pH 7.0, 0.1 M NaCl, and 0.2 mM EDTA with 2% DMSO; (b) **5**, 2×10^{-5} M, in the presence of oligonucleotide TA, 4.56×10^{-5} M; (c) subtraction of spectrum 2a from spectrum 2b.

temperature. The three-lines spectra obtained for both compounds (16 G splitting) result from anisotropic interaction between the unpaired electron and the nuclear spin of the nitrogen atom. The spectra are characteristic of nitroxide radicals undergoing relatively rapid motion (Figures 1a and 2a). Kivelson's equation was used exclusively to calculate τ_c of the free species in buffered aqueous solution. From the relative peak heights and using Kivelson's equation, rotational correlation times $\tau_c = 1.3 \times 10^{-10}$ s and $\tau_c = 9 \times 10^{-11}$ s were calculated for molecules **3** and **5**, respectively; $\tau_c = 9 \times 10^{-11}$ s is within the range of values generally observed for tricyclic intercalating agents (*32*, *37*). The higher correlation time observed for the adenine−acridine conjugate **3** is in accordance with the larger size of the molecule compared to **5**.

In the presence of the natural TA oligonucleotide duplex, the spectra of the two molecules exhibit identical changes (Figures 1b and 2b) that are interpreted as resulting from the addition of two spectra: that of a new immobilized species which superimposes to that of the radical free in solution. Subtraction of the spectra corresponding to the free species from the experimental gives for the two molecules a broad and asymmetric spectrum (Figures 1c and 2c) characteristic of species undergoing restricted motion (indeed, identical spectra corresponding exclusively to the same immobilized species were obtained when operating at low drug-to-oligonucleotide ratios and at relatively high concentrations of duplex). The spectra are similar for the two labeled molecules **3** and **5**. A rotational correlation time $\tau_c = 3 \times 10^{-9}$ s was calculated for the two systems using Kuznetsov's method. This is a crude value, keeping in mind the isotropic motion approximation. These spectra and the corresponding τ_c value can be confidently ascribed to the intercalated form of the labeled acridine. Aminoacridines are well-known DNA intercalators that have been the object of numerous studies, and we have recently reported *(43)* that the association constant of the labeled propylamino acridine **5** for calf thymus DNA, $K = 3 \times 10^4$ M^{-1}, differs only slightly from that of the unlabeled analogue **4**, $K = 6.4 \times 10^4$ M^{-1}. This strongly favors the hypothesis of an identical intercalative mode of interaction for the labeled and unlabeled molecules. Due to weak solubility of **5**, it was not possible to measure the affinity constant with the TA duplex. By double integration of the EPR spectra corresponding to the intercalated form of the conjugate **3**, we obtained experimental data which were fitted according to the McGhee and Von Hippel treatment *(49);* the association constant for the undecamer TA duplex was calculated as $K_{TA} = 4 \times 10^4$ M^{-1}, with $n = 2$, where n is the number of excluded sites (Figure 3a).

*Interaction of **3** with the Abasic TX Duplex.* The EPR spectra of molecules **3** and **5** were equally measured in the presence of the TX duplex that contains the abasic site X opposite to a thymine base. The results are quite different for the two molecules. The EPR spectrum registered for molecule **3** that contains the adenine recognition moiety corresponds to an addition spectrum of up to three species: (i) the radical free in solution; (ii) the radical intercalated in DNA similar to that observed in the interaction with the TA duplex in the preceding experiment; and (iii) a new more immobilized form that was identified as the "abasic site-bound species" (see further in the text).

Figure 4a shows, for example, the spectrum registered for molecule **3** present in excess relative to the TX duplex. Subtraction of the spectrum characteristic of the free species gives Figure 4b from which the spectrum of the intercalated drug can be subtracted to give Figure 4c characteristic of the "abasic site bound" form. Using Kuznetsov's treatment, a rotational correlation time $\tau_c = 6 \times 10^{-9}$ s was determined (the value was indeed calculated from an accumulate spectrum due to the noisy character of spectrum 4c). It must

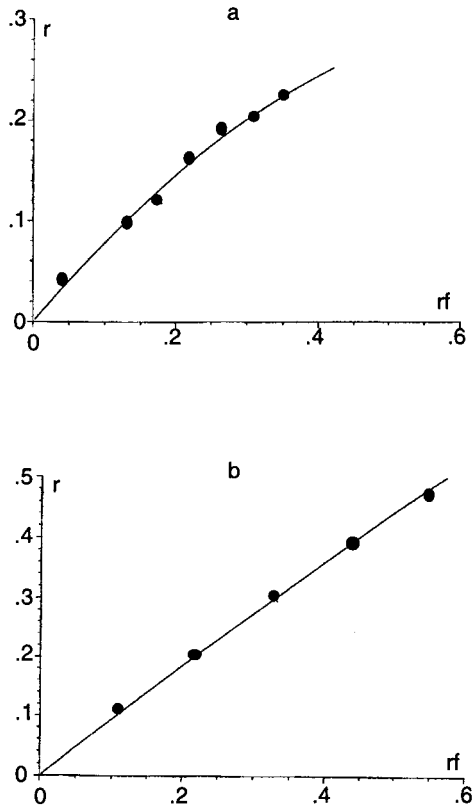

FIGURE 3: McGhee and Von Hippel treatment. r = ratio of bound drug per oligonucleotide as a function of rf (=ratio of total drug per oligonucleotide). (a) TA duplex, concentration expressed in base pairs: 1.13×10^{-5} M; (b) TX duplex, concentration expressed in moles of duplex, i.e., in abasic site: 0.91×10^{-5} M.

be considered as a rough value as a consequence of the isotropic motion approximation.

Analysis of the spectra registered in different conditions of concentration and at different drug-to-oligonucleotide ratios r allows quantitative determination of the forms present in solution. At low ratios $r \leq 0.4$, the "abasic site specific" form is the sole immobilized species, accompanied or not, depending on the concentrations, by the free species. Figure 4d shows, for example, the spectrum registered at low ratio $r = 0.21$ and at "relatively" high concentration in TX duplex (2.35×10^{-5} M). This spectrum is that of the abasic site-specific form only. It is similar to spectrum 4c obtained from two successive subtractions (the sole difference resides in the lower intensity of the signal in the subtraction spectrum 4c, that reflects only a fraction of the radical in solution). At higher ratios, $r \geq 0.6$, contribution of the intercalated and free species to the experimental spectrum is clearly observable. Double integration of the spectra corresponding to the "AP-site specific" form (i.e. the spectra are registered at concentrations where the latter species is the sole form present in solution with the free form) allows determination of the association constant of drug **3** for the duplex, $K_{TX} = 1.5 \times 10^6$ M^{-1}, $n = 1$ (Figure 3b). This value measures the binding of the drug at the abasic site specifically. This value, which is 40 times higher than the affinity constant measured for duplex TA ($K_{TA} = 4 \times 10^4$ M^{-1}), reflects the high tendency of molecule **3** to bind selectively to the abasic site rather than intercalate between any of the base pairs in the duplex. We looked for possible displacement of the drug by the triaminopurine derivative **6** that possesses both a

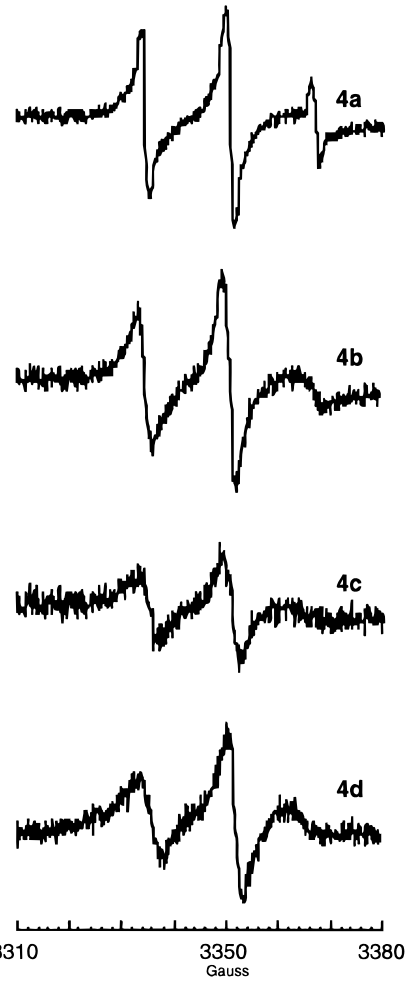

FIGURE 4: EPR spectra of (a) **3**, 1.5×10^{-5} M, in the presence of oligonucleotide TX, 0.91×10^{-5} M ($r = 1.65$), 25 mM Tris-HCl, pH 7.0, 0.1 M NaCl, and 0.2 mM EDTA with 2% DMSO; (b) subtraction of spectrum 1a (corresponding to **3** free in the buffer) from spectrum 3a; (c) subtraction of spectrum 1c (corresponding to **3** intercalated) from Figure 3b; (d) **3**, 0.5×10^{-5} M, in the presence of oligonucleotide TX, 2.36×10^{-5} M ($r = 0.21$).

polyamino chain to interact ionically with the phosphate backbone and an adenine moiety to insert into the abasic pocket and pair with the opposite thymine. No change in the spectra was observed on addition of a 50-fold excess of **6**.

All these data can be compared to the results obtained by the high-field NMR study of the unlabeled analogue **1** with the same TX oligonucleotide. This study performed at a one-to-one ratio of drug per duplex molecule, at 10^{-3} M concentration, had shown that the drug binds at the abasic site exclusively (at the precision of the NMR technique) with the base inserted in the abasic pocket and the acridine intercalated at a two base pair distance 5′ to the abasic site in two geometries corresponding to a 180° rotation of the acridine unit around the C9−N bond, positioning the $-OCH_3$ group alternatively in the minor groove for the major complex (70%) and in the major groove for the minor complex (30%).The most immobilized form observed in the present study that was identified as "the abasic site-bound" species can most probably be ascribed to these complexes evidenced by NMR.

Molecular modeling calculations were performed to ascertain this hypothesis and evaluate the modifications brought

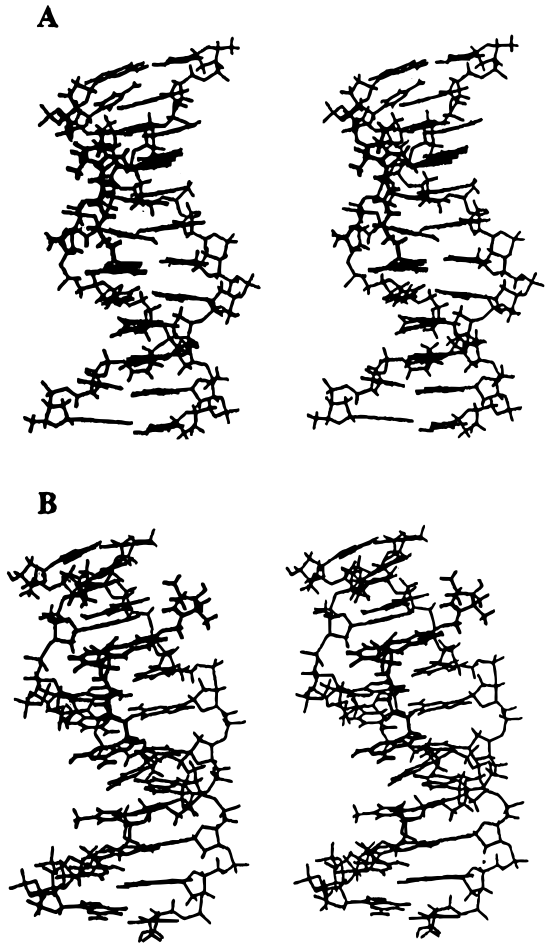

FIGURE 5: Stereoview of the model for the **3**−DNA complex in the Hoogsteen conformation with the label part protruding in the minor (A) or major groove (B). Molecule **3** is shown in boldface lines.

by the nitroxide label to the geometry of the complexes. The structures of the complexes formed between the unlabeled molecule **1** and the abasic duplex derived from 2-D ^{1}H NMR were used to predict the interactions of the spin-label with DNA. The N−O spin-label was modeled as the hydroxylamine *(50)*. The methyl group of acridine was replaced by the methylene pyrroline-1 hydroxy substituent in the two configurations observed in the NMR, i.e., with the label protruding in the minor groove (major complex) and in the major groove (minor complex). The energy was then minimized. Figure 5 is a stereoview of the two complexes. Inspection of the model led us to conclude that the attachment of the relatively bulky spin-label would not introduce steric clashes with the surrounding DNA for the two complexes. The situation is energetically slightly more favorable when the label is in the minor groove where interactions with the walls of the DNA duplex induce no conformational distortion. The rigid five-membered unsaturated nitroxide-bearing ring is expected to have only slight internal conformational mobility in the complex relative to the acridine ring. On the other hand, when the label is located in the major groove, we may expect a motion of the spin-label independent of the motion of DNA itself.

To evaluate the motion of the label in the complex relative to that of the DNA duplex, we calculated the theoretical correlation time for the overall motion of the duplex. The

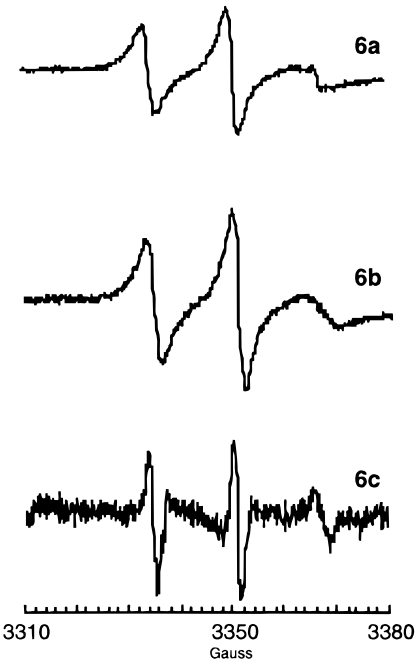

FIGURE 6: EPR spectra of (a) **5**, 2×10^{-5} M, in the presence of oligonucleotide TX, 4.55×10^{-5} M, in the buffer; (b) subtraction of Figure 2a (corresponding to **5** free in the buffer) from Figure 5a; (c) subtraction of Figure 2c (corresponding to **5** intercalated) from Figure 5b.

rotational correlation time of a spherical molecule *(51)* is given by $\tau_c = V(n/kT)$, where V is the hydrated volume and η is the viscosity of the medium. This equation is generally used to calculate τ_c values for small DNA oligomers although it gives only crude values due to the poor approximation of the sphere model. The hydrated volume for the duplex oligonucleotide was calculated with the rigid-cylinder formula *(48, 30)*. A theoretical value $\tau_c = 5.8 \times 10^{-9}$ s was thus obtained that can be compared to the experimental value $\tau_c = 6 \times 10^{-9}$ s extracted from the spectrum. Keeping in mind the approximation of the calculation, good agreement is obtained between the calculated movement of the abasic duplex and the experimental motion of the label. This suggests that the rotational freedom of the nitroxide group is limited by its complexation within the oligonucleotide and that its movement is close to that of the duplex, in accordance with the results of molecular modeling.

*Interaction of **5** with the Abasic Duplex.* The spectrum of the labeled propylaminoacridine **5** was monitored in the presence of the abasic duplex. Figure 6a shows the spectrum registered at a drug-to-oligonucleotide ratio $r = 0.44$. The spectrum is again an addition spectrum from which the different components were analyzed by successive subtractions as was done previously. In the range of concentrations used (4.55×10^{-5} M in duplex oligonucleotide), the major species present in solution (85−90%) is the intercalated form characterized previously in the interaction of the drug with the natural duplex ($\tau_c = 3 \times 10^{-9}$ s) accompanied by a very minor proportion of the free species estimated to ca. 3%. A new species, not observed in the preceding experiments, accounts for ca. 10% of the total (Figure 6c). This value is appreciated with poor precision as it is difficult to quantitate species with similar line shapes in the fast motional domain. In addition, Figure 6c is a difference spectrum corresponding to a species of intermediate mobility and present in a small

amount,which accounts for its poor character. Nevertheless, it shows relatively sharp lines indicating less retarded motion, from which the rotational correlation time was calculated using Kivelson's equation, $\tau_c = 6 \times 10^{-10}$ s. On adding the triaminopurine derivative **6** (50-fold excess relative to drug **5**), a new spectrum was obtained which after subtraction of the intercalated species gave a base line. The new species is thus totally displaced from the oligonucleotide. The interpretation of the data is that the labeled acridine interacts nonspecifically between the base pairs in the usual intercalative manner as observed in the interaction with the natural duplex. The complexes are characterized by $\tau_c = 3 \times 10^{-9}$ s. However, a small proportion of the drug inserts into the abasic site, forming a weakly immobilized complex identified by a lower rotational correlation time, $\tau_c = 6 \times 10^{-10}$ s. It seems reasonable to postulate that this complexation corresponds to partial insertion of the acridine into the abasic pocket with only partial stacking of the acridine ring between the flanking bases. One can anticipate high rotational freedom of the nitroxide label and weak stability for such a complex, which can explain both the small rotational correlation time observed and the displacement of the drug by the triaminopurine molecule **6**.

These observations mean notably that the abasic site constitutes a binding site for the propylaminoacridine intercalator **5**. However, the proportion of drug molecules bound to this site (ca. 10% in the conditions of the experiment Figure 6) compared to the intercalated molecules in equilibrium between the different intercalation sites in the duplex (85−90%) does not suggest any marked preference for any site (taking into account the statistical factor that measures the number of intercalation sites vs abasic site in the undecamer duplex).

DISCUSSION

With the ultimate goal of studying base excision repair (BER) inhibition by drugs that specifically bind to abasic sites in DNA and may thus potentiate the action of antitumor drugs that create multiple abasic damage in cells, we have examined by EPR spectroscopy the interaction of the spin-labeled acridine−adenine conjugate **3** with a duplex oligonucleotide containing a stable analogue of the abasic site. The labeled conjugate **3** is an analogue of the drug **1** that had been shown previously by T_m measurements and high-field NMR spectroscopy to bind selectively at the abasic site. For better interpretation of the EPR data, we also studied the interaction of **3** with the parent unmodified TA duplex and compared the behavior of this labeled conjugate **3** to that of the aminoacridine subunit **5**.

The labeled conjugate **3** exhibits in water an EPR spectrum characteristic of a nitroxide radical undergoing relatively rapid motion ($\tau_c = 1.3 \times 10^{-10}$ s). As expected, this value is slightly higher than that exhibited by the propylaminoacridine subunit **5** ($\tau_c = 9 \times 10^{-11}$ s). The conjugate **3** binds to "normal" DNA (TA duplex), forming a complex characterized by an important mobility decrease of the nitroxide label. The complex most probably involves intercalation of the acridine moiety as the spectra are similar to those observed for the propylaminoacridine subunit **5**. In the presence of abasic DNA (TX duplex) and depending on the concentrations and on the drug-to-oligonucleotide ratio used, the conjugate **3** may exist as three different forms: (i) the radical free in solution; (ii) the intercalation complex already identified and characterized in the interaction with "normal" DNA; and (iii) the abasic site-specific complex which is the most immobilized form and which is the major form observed at a 1:1 ratio of drug per oligonucleotide and at the highest concentrations. All data indicate that it corresponds to the complex observed by high-field NMR spectroscopy for the parent unlabeled conjugate **1** interacting with the same abasic duplex. In this complex, the three subunits of the conjugate are ideally located for interaction, the acridine intercalates with the amino group protruding in the minor groove, the polyamino linker extends in the minor groove, and the adenine base locks inside the abasic pocket facing thymine in the opposite strand probably in the Hoogsteen mode. Molecular modeling and calculation of an approximate correlation time suggest that the geometry of the complex is not significantly modified by the nitroxide label and rotation of the label is restricted. The structural complementarity between the conjugate drug and the abasic DNA accounts for the restricted mobility and for the high association constant of the drug at the abasic site. It also accounts for the fact that the conjugate is not displaced from the abasic duplex by a 50-fold excess of triaminoadenine **6**. All these data point to the role of the adenine unit in the conjugate **3** to direct the binding selectively at the abasic site facing thymine in the opposite strand.

The comparison with the behavior of the triaminoacridine derivative **5** that possesses the acridine and polyamino subunits present in **3**, but is devoid of the adenine base, is instructive. The molecule binds at the abasic site and also at the intercalation sites. The complex at the abasic site shows increased mobility compared to the intercalated species. It is displaced from the abasic duplex on addition of a 50-fold excess of the triaminoacridine **6**.

It is interesting to note that EPR spectrocopy furnishes information on the number and dynamics of species in interaction with the DNA duplex that is remarkably in accordance and complementary to the data extracted from the T_m measurements in the UV and from high-field NMR spectroscopy and restrained molecular dynamics. The NMR study of the interaction of conjugate **3** with the abasic duplex was monitored at a 1:1 ratio, requiring relatively high concentrations of material ($\approx 10^{-3}$ M). Very precise information was extracted about the geometry of the complex to the extent that essentially one single complex exists in these conditions. EPR spectrocopy, on the other hand, requires low concentrations in drug and DNA so that a large number of spectra could be registered allowing variations in a range of concentrations and ratios. This permitted identification and quantitative evaluation of up to three species present in solution: the conjugate free in solution, the "intercalation complex", and the "abasic site-specific complex". This was possible as each individual species in solution is characterized by a different rotational correlation time. This opens the possibility of studying the interaction of the labeled conjugate **3** with different abasic DNA duplexes possessing the different nucleotide bases opposite the abasic site to evaluate the specificity of the recognition of the abasic site by the base of the drug. This study is currently under way. Such studies constitute the structural basis to further evalutate the interest of such conjugates of general structure "base−chain−

intercalator" to recognize specifically the abasic site in DNA and interfere with the repair process of the abasic damage.

ACKNOWLEDGMENT

We thank A. Jeunet for technical assistance in EPR; Dr. P. Belmont, Dr. M. Demeunynck, and Dr. J. F. Constant for the labeled products and oligonucleotides; and Dr. C. Coulombeau for molecular modeling calculations.

REFERENCES

1. Loeb, L., and Preston, B. (1986) *Annu. Rev. Genet. 20*, 201−230.
2. Lindahl, T., and Nyberg, B. (1972) *Biochemistry 11*, 3610−3618.
3. Greer, S., and Zamenho, F. S. (1992) *J. Mol. Biol. 4*, 123−141.
4. Von Sonntag, C. (1987) in *The Chemical Basis of Radiation Biology*, pp 221−294, Taylor and Francis, London.
5. Lown, J. W., and McLaughlin, L. W. (1979) *Biochem. Pharmacol. 28*, 1631−1638.
6. Bailly, V., and Verly, W. G. (1989) *Nucleic Acids Res. 17*, 3617−3618.
7. Demple, B., and Harrison, L. (1994) *Annu. Rev. Biochem. 63*, 915−948.
8. Larson, K., Sahm, J., Schenkar, R., and Strauss, B. (1985) *Mutat. Res. 150*, 77−84.
9. Boiteux, S., and Laval, J. (1982) *Biochemistry 21*, 6746−6751.
10. Hickson, I. D. (1997) in *Base Excision Repair of DNA Damage*, pp 81−102, Springer-Verlag, Heidelberg, Germany.
11. Constant, J. F., Fkyerat, A., Demeunynck, M., Laval, J., O′Connor, T. R., and Lhomme, J. (1988) *Nucleic Acids Res. 16*, 2691−2703.
12. Constant, J. F., Fkyerat, A., Demeunynck, M., Laval, J., O′Connor, T. R., and Lhomme, J. (1990) *Anti-Cancer Drug Des. 5*, 59−62.
13. Fkyerat, A., Demeunynck, M., Constant, J. F., Michon, P., and Lhomme, J. (1993) *J. Am. Chem. Soc. 115*, 9952−9959.
14. Fkyerat, A., Demeunynck, M., Constant, J. F., and Lhomme, J. (1993) *Tetrahedron 49*, 11237−11252.
15. Berthet, N., Boudali, A., Constant, J. F., Decout, J. L., Demeunynck, M., Fkyerat, A., Garcia, J., Laayoun, A., Michon, P., and Lhomme, J. (1994) *J. Mol. Recognit. 7*, 99−107.
16. Belmont, P., Boudali, A., Constant, J. F., Demeunynck, M., Fkyerat, A., Lhomme, J., Michon, P., and Serratrice, G. (1997) *New J. Chem. 21*, 47−54.
17. Barret, J. M., Fahy, J., Ethiévant, C., Lhomme, J., Hill, B. T. (1999) *Anticancer Drugs 10*, 55−65.
18. Coppel, Y., Berthet, N., Constant, J. F., Coulombeau, C., Coulombeau, Ce., Garcia, J., and Lhomme, J. (1997) *Biochemistry 36*, 4817−4830.
19. Coppel, Y., Constant, J. F., Coulombeau, C., Demeunynck, M., Garcia, J., and Lhomme, J. (1997) *Biochemistry 36*, 4831−4843.
20. Berthet, N., Constant, J. F., Demeunynck, M., Michon, P., and Lhomme, J. (1997) *J. Med. Chem. 40*, 3346−3352.
21. Dugas, H. (1977) *Acc. Chem. Res. 10*, 47−54.
22. Bobst, A. M. (1979) in *Spin Labeling II: Theory and Applications* (Berliner, L. J., Ed.) pp 291−342, Academic Press, New York.
23. Bobst, A. M., Kao, S. C., Toppin, R. C., Ireland, J. C., and Thomas, I. E. (1984) *J. Mol. Biol. 173*, 63−74.
24. Kao, S. C., and Bobst, A. M. (1985) *Biochemistry 24*, 5465−5469.
25. Pauly, G. T., Thomas, I. E., and Bobst, A. M. (1987) *Biochemistry 26*, 7304−7310.
26. Spaltenstein, A., Robinson, B. H., and Hopkins, P. B. (1989) *Biochemistry 28*, 9484−9495.
27. Kirchner, J. J., Hustedt, E. J., Robinson, B. H., and Hopkins, P. B. (1990) *Tetrahedron Lett. 31*, 593−596.
28. Hustedt, E. J., Spaltenstein, A., Kirchner, J. J., Hopkins, P. B., and Robinson, B. M. (1993) *Biochemistry 32*, 1774−1787.
29. Hustedt, E. J., Kirchner, J. J., Spaltenstein, A., Hopkins, P. B., and Robinson, B. M. (1995) *Biochemistry 34*, 4369−4375.
30. Keyes, R. S., and Bobst, A. M. (1995) *Biochemistry 34*, 9265−9276.
31. Fischhaber, P. L., Reese, A. W., Nguyen, T., Kirchner, J. J., Hustedt, E. J., Robinson, B. H., and Hopkins, P. B. (1997) *Nucleosides Nucleotides 16*, 365−377.
32. Spielmann, H. P., Chi, D. Y., Hunt, N. G., Klein, M. P., and Hearst, J. E. (1995) *Biochemistry 34*, 14801−14814.
33. (a) Spaltenstein, A., Robinson, B. H., and Hopkins, P. B. (1989) *J. Am. Chem. Soc. 111*, 2303−2305. (b) Strobel, O. K., Keyes, R. S., and Bobst, A. M. (1990) *Biochemistry 29*, 8522−8528.
34. Miller, T. R., Alley, S. C., Reese, A. W., Solomon, M. S., McCallister, W. V., Mailer, C., Robinson, B. H., and Hopkins, P. B. (1995) *J. Am. Chem. Soc. 117*, 9377−9378.
35. Bernier, J. L., Henichart, J. P., and Catteau, J. P. (1981) *Anal. Biochem. 117*, 12−17.
36. Bernier, J. L., Henichart, J. P., and Catteau, J. P. (1981) *Biochem. J. 199*, 479−484.
37. Robinson, B. H., Lerman, L. S., Beth, A. H., Frisch, H. L., Dalton, L. R., and Auer, C. (1980) *J. Mol. Biol. 139*, 19−44.
38. Hurley, L., Osei-Gyimah, P., Archer, S., Scholes, C. P., and Lerman, L. S. (1982) *Biochemistry 21*, 4999−5009.
39. Carrier, A., Le Ber, P., and Auclair, C. (1990) *Biochemistry 29*, 6002−6009.
40. Ottaviani, M. F., Ghatlia, N. D., Bossmann, S. H., Barton, J. K., Dürr, H., and Turro, N. J. (1992) *J. Am. Chem. Soc. 114*, 8946−8952.
41. Hong, S.-J., and Piette, L. H. (1976) *Cancer Res. 36*, 1159−1171.
42. Hong, S.-J., and Piette, L. H. (1978) *Arch. Biochem. Biophys. 185*, 307−315.
43. Belmont, P., Chapelle, C., Demeunynck, M., Michon, J., Michon, P., and Lhomme, J. (1998) *Bioorg. Med. Chem. Lett. 8*, 669−674.
44. Kivelson, D. (1960) *J. Chem. Phys. 33*, 1094−1106.
45. Libertini, L. J., and Griffith, O. H. (1970) *J. Chem. Phys. 53*, 1359−1367.
46. Kuznetsov, A. N., Wasserman, A. M., Volkov, A. Ju., and Korst, N. N. (1971) *Chem. Phys. Lett. 12*, 103−106.
47. The nitroxide motion consists of both global and internal contributions. The internal dynamics are characterized by an order parameter and an internal correlation time describing a spin label rapidly diffusing within the slowly tumbling oligomer. See, for example, reference 30 and references cited therein.
48. Tirado, M. M., and Garcia de la Torre, J. (1980) *J. Chem. Phys. 73*, 1986−1993.
49. McGhee, J. D., and Von Hippel, P. H. (1974) *J. Mol. Biol. 86*, 469−489; (1976) *J. Mol. Biol. 103*, 679.
50. See, for example, ref *32*.
51. Bloembergen, N., Purcell, E. M., and Pound, R. V. (1948) *Phys. Rev. 73*, 679−712.

BI981770E